nature publishing group

Early tissue transglutaminase–mediated response underlies K562(S)-cell gliadin-dependent agglutination

Marco Silano[1], Olimpia Vincentini[1], Alessandro Luciani[2], Cristina Felli[1], Sergio Caserta[3], Speranza Esposito[2], Valeria Rachela Villella[3], Massimo Pettoello-Mantovani[2], Stefano Guido[3] and Luigi Maiuri[2]

INTRODUCTION: K562(S) agglutination has been used as a rapid and economic tool for the *in vitro* screening of the toxicity of cereal fractions and prolamins in celiac disease (CD). A strict correlation has been reported between the toxicity of cereals and cereal fractions for celiac patients and their ability to agglutinate K562(S) cells. Whether this specificity of K562(S)-cell agglutination is caused by the activation of the same pathogenic events triggered by toxic cereal fractions in CD intestine or simply represents a bystander event of gluten toxicity is, however, unknown.

METHODS: K562(S) cells were incubated *in vitro* with the peptic-tryptic digest of wheat gliadin.

RESULTS: The agglutination of K562(S) cells by wheat gliadin peptides is orchestrated by a cascade of very early events occurring at the K562(S)-cell surface similar to those occurring at the intestinal epithelial surface. They involve a rapid increase in intracellular calcium levels that activate tissue transglutaminase (TG2), leading to a rapid actin reorganization that is pivotal in driving cell agglutination. These specific effects of toxic cereals are phenocopied by the gliadin-derived peptide p31–43, which orchestrates the activation of innate response to gliadin in CD.

DISCUSSION: Our study provides the rationale for the extensive use of K562(S)-cell agglutination as a valuable tool for screening cereal toxicity.

Celiac disease (CD) is a permanent intolerance to gluten, an alcohol-soluble protein fraction present in some cereals such as wheat, rye, and barley, occurring in genetically predisposed individuals (1,2). During the past few years, a series of seminal papers have provided a clearer picture of the pathogenic mechanisms of CD with a specific activation by gluten/gliadin-derived peptides of HLA (histocompatibility leukocyte antigen)-DQ 2/8 restricted $CD4^+$ T cells at the small-intestinal level (3). Despite this unassailable evidence, a series of studies have indicated that T cells, although essential for the full CD manifestation, cannot explain all the facets of CD (4,5). These studies have suggested that different portion(s) of gliadin, ostensibly not the ones recognized by T cells, modulate an innate activation of celiac small intestine that sets the tone and intensity of the adaptive immune response induced by the immunodominant gliadin epitopes (6). Surprisingly, gliadin and prolamin preparations also show biological activity on celiac-unrelated *in vitro* systems, including intestinal epithelial cells lines, fetal rat jejunum, and K562(S) cells, a highly undifferentiated cell line isolated from an outgrowth of a patient with chronic myelogenous leukemia (7–9). K562(S) cells undergo agglutination within few minutes after contact with gluten digests. A strict correlation has been reported between the toxicity of cereals and cereal fractions for celiac patients and their biological activity in these unrelated *in vitro* systems (10). Therefore, the ability to agglutinate K562(S) cells has been used for screening of toxicity of gluten fractions belonging to different cultivars (11). The mechanisms underlying such a puzzling behavior of toxic cereal fractions are unknown. In particular, this evidence raised a series of issues; the most pressing is the clarification of where the specificity for gliadin of these unrelated models lies. A common feature of gliadin/prolamin response between gluten/gliadin-responsive intestinal epithelial cell lines, such as T84, and the K562(S) model is the rapidity of response. Indeed, K562(S) cell agglutination is a very rapid event (11), and gliadin digests are able to upregulate tissue transglutaminase (TG2) protein and activity as well as induce cytoskeleton reorganization (12) very early upon gluten/gliadin exposure in sensitive epithelial cells. Moreover, neutralizing such precocious events is effective in controlling the downstream gliadin-triggered epithelial activation (13). Whether these mechanisms also underlie the agglutination of K562(S) cells is, however, still unknown.

Here, we demonstrate how the agglutination of K562(S) cells by gliadin preparation or gliadin-derived peptides is induced by a cascade of very precocious events occurring at the cell surface upon contact with toxic gluten fractions and involves surface mechanisms similar to those induced in intestinal epithelial cells.

RESULTS

PT Gliadin Digest Induces Very Early TG2 Activation in K562(S) Cells Upon Gliadin Exposure

TG2 is a Ca^{2+}-dependent ubiquitous enzyme with multifaceted functions that mainly catalyzes deamidation or cross-linking of substrate proteins via ε-(γ-glutamyl)lysine isopeptide bonds (14,15). TG2 is also involved in cytoskeleton rearrangement (14). Because TG2 plays a key role in the most precocious

[1]Unit of Human Nutrition and Health, Istituto Superiore di Sanità, Rome, Italy; [2]Institute of Pediatrics, University of Foggia, Foggia, Italy; [3]Department of Chemical Engineering, University of Napoli Federico II, Naples, Italy. Correspondence: Marco Silano (marco.silano@iss.it)

Received 06 July 2011; accepted 13 December 2011; advance online publication 7 March 2012. doi:10.1038/pr.2012.4

events triggered by gliadin both in celiac duodenum and in gliadin-sensitive intestinal epithelial cells (13,16,17), we examined whether peptic tryptic (PT) digests from gliadin, able to agglutinate K562(S) cells, could upregulate TG2 protein. As control, we used zein PT digest, nontoxic for celiac patients and unable to agglutinate K562(S) cells (18). Western blot analysis revealed that K562(S) cells constitutively express high TG2 protein levels (**Figure 1**) regardless of gliadin stimulation. Next, we investigated whether PT gliadin digest could upregulate TG2 activity. The analysis of biotinylated monodansylcadaverine incorporation by confocal microscopy revealed that only PT gliadin, but not zein, digests were highly effective in inducing a marked increase in TG2 activation, together with K562(S) agglutination (**Figure 2a–c**). The relationship between TG2 activation and cell agglutination was confirmed by the evidence that the anti-TG2 antibody CUB 7402, which neutralizes TG2 activation (19), prevented gliadin-induced K562(S) agglutination (agglutination velocity: gliadin PT digest, 0.8 ± 2.0 vs. gliadin PT digest + CUB 7402, 11.6 ± 0.8; $P < 0.05$).

The lack of TG2 cross-linking activity in spite of the high protein contents in unstimulated K562(S) cells suggests that agglutinating PT digests could be endowed with the ability to induce an early increase in intracellular Ca^{2+} levels. Indeed, TG2 cross-linking activity is strictly regulated by Ca^{2+} levels, and the Ca^{2+}-binding molecule ethyleneglycol-bis(baminoethylether)-*N,N9*-tetraacetic acid prevents cell agglutination (20). Accordingly, K562(S) cells are usually grown in a Ca^{2+}-free medium (10,11). Therefore, we investigated the effects of increasing Ca^{2+} concentrations in the culture medium on K562(S) agglutination. In fact, TG2 is activated by a concentration of Ca^{2+} higher than 1–2 mmol/l (21,22). As shown in **Figure 3a**, Ca^{2+} concentrations below 1 mmol/l were not able to induce K562(S) agglutination, whereas Ca^{2+} levels higher than 2 mmol/l induced massive agglutination. Moreover, the concomitant exposure of K562(S) cells to 2 mmol/l Ca^{2+} and the anti-TG2 antibody CUB7402 prevented Ca^{2+}-induced cell agglutination (optical density 2.1 for cells exposed to Ca^{2+} 2 mmol/l alone vs. 9.9 for cells exposed to Ca^{2+} 2 mmol/l and CUB7402). Therefore, we investigated whether PT gliadin digest could increase intracellular Ca^{2+} levels in K562(S) agglutinated cells. We found that PT gliadin digest induced a dramatic increase in the intracellular Ca^{2+} levels within 5 min of incubation, whereas PT zein digest or phosphate-buffered saline (PBS) did not (**Figure 3b,c**). L,2-bis(aminophenoxy) ethane-N,N,N,N′-tetraacetic acid (BAPTA)-AM (5 mmol/l), a Ca^{2+} chelator also prevented both PT gliadin-induced TG2 activation (data not shown) and agglutination in K562(S) cells (**Figure 3d**). Furthermore, ionomycin (5 mmol/l) induced K562(S) agglutination (data not shown). Together, these findings demonstrate that PT digests from toxic cereals agglutinate K562(S) cells by inducing an early increase in intracellular Ca^{2+} levels, leading to TG2 activation.

Next, we addressed whether such an early Ca^{2+}-dependent TG2 activation, occurring in K562(S) cells upon gliadin exposure, could also regulate the rearrangement of cytoskeleton that is pivotal in cell agglutination (23,24). Blocking TG2 activation, a central player of these cell surface events (14), by means of the Ca^{2+} chelator BAPTA-AM or the anti-TG2 antibody CUB 7402 prevented the early rearrangement of the actin fibers occurring after a few minutes of gliadin challenge (**Figure 4a**).

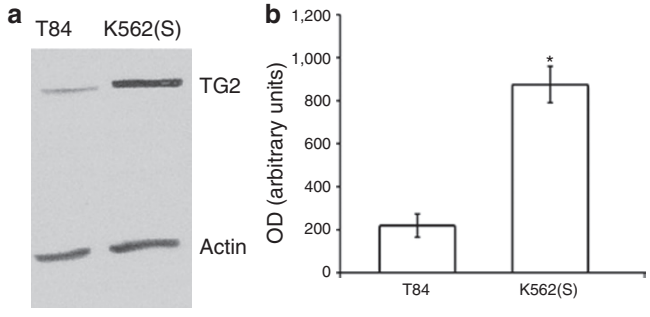

Figure 1. Transglutaminase 2 (TG2) basal level in K562(S) and T84 cells (without gliadin stimulation). (**a**) A western blot representative of the three experiments performed. (**b**) Quantification of TG2 expression in cells. Values are expressed as mean ± SEM normalized for the actin in densitometry arbitrary units of three different experiments, each performed in triplicate ($n = 9$). Statistical analysis was performed by Wilcoxon test vs. T84 cells (*$P < 0.05$). OD, optical density.

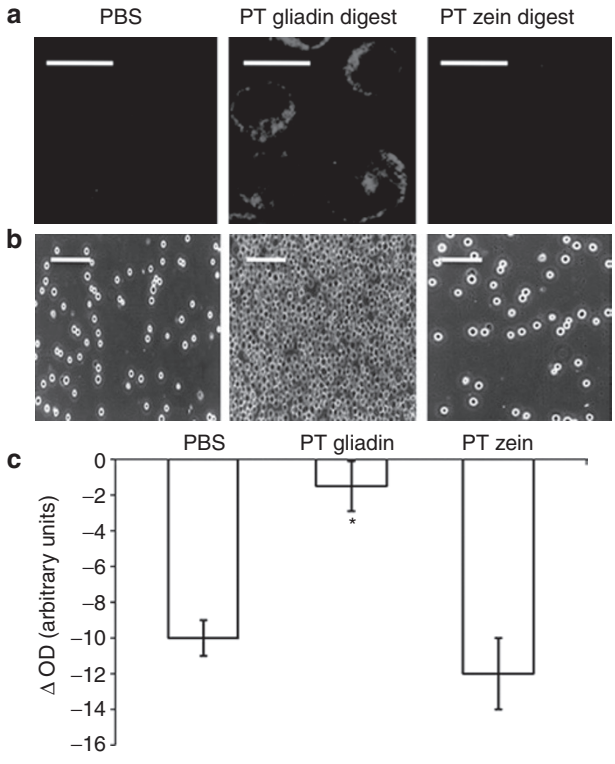

Figure 2. PT digest of gliadin, but not zein, induces K562(S) TG2 activation and cell agglutination. (**a**) PT gliadin digest induced TG2 activity (red; color image available online) in K562(S) agglutinated cells. Confocal microscopy. Bars = 25 µm. (**b**) Light microscopy of K562(S) cells after 30-min incubation with medium and PT digest of gliadin and of zein. Bars = 100 µm. (**c**) Measurement of agglutination velocity. Results are expressed as mean ± SEM of three independent experiments, each performed in triplicate ($n = 9$). Statistical significance (*$P < 0.05$) was calculated by Wilcoxon results vs. cells incubated with PBS alone. OD, optical density; PBS, phosphate-buffered saline; PT, peptic tryptic; TG2, transglutaminase 2.

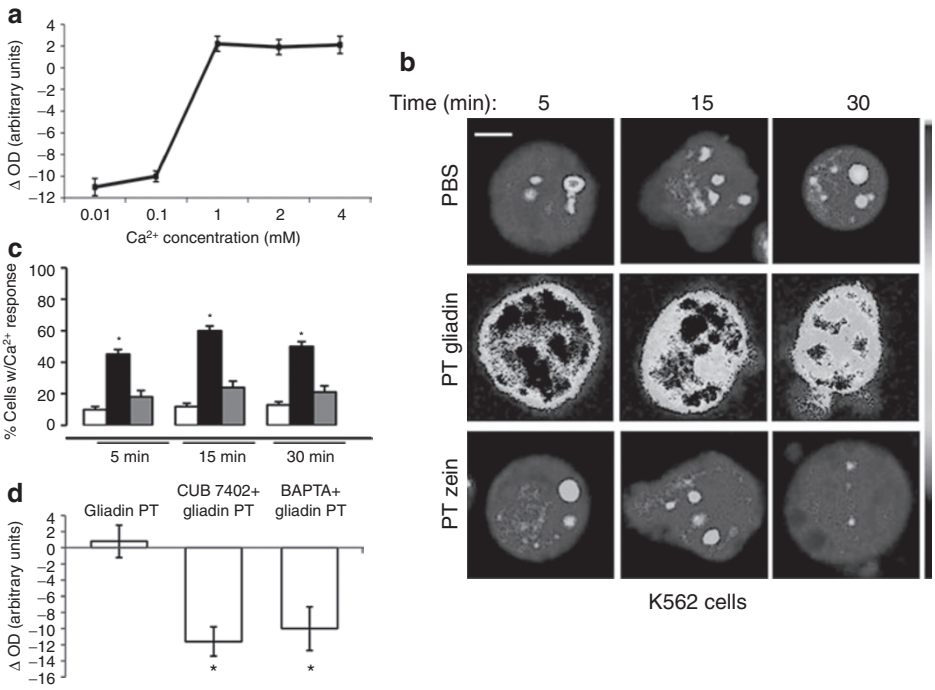

Figure 3. Increased intracellular Ca^{2+} levels are necessary for the agglutination of K562(S) cells. (**a**) Titration curve of CaCl (mmol/l) added to culture medium in relation to the agglutination velocity. (**b**) Imaging with Fura of Ca^{2+} intracellular levels in K562(S) cells exposed to gliadin and zein PT digests and culture medium alone. Colors correspond to the scale of $[Ca^{2+}]i$ increase (color image available online). Red, high $[Ca^{2+}]i$ contents. Bar = 10 µm. (**c**) K562(S) cells were exposed to PBS (open bars), PT gliadin (black bars), or PT zein (gray bars) for up to 30 min and after Ca^{2+} imaging pseudocolor ratiometric images with Fura-2 were acquired. Quantification of results from three independent experiments ($n = 9$) is shown in the histogram. *$P < 0.001$ vs. samples cultured with gliadin-derived peptide 31–43. (**d**) Measurement of agglutination velocity of K562(S) cells exposed to neutralizing anti-TG2 antibody CUB 7402 and the Ca^{2+} chelator BAPTA-AM. Results are expressed as mean ± SEM of three independent experiments ($n = 9$), each performed in triplicate. Statistical significance (*$P < 0.05$) was calculated by Wilcoxon results vs. cells incubated with PBS alone. $[Ca^{2+}]i$, intracellular calcium; BAPTA, L, 2-bis(aminophenoxy)ethane-N,N,N,N′-tetraacetic acid; OD, optical density; PBS, phosphate-buffered saline; PT, peptic tryptic; TG2, transglutaminase 2.

Gliadin-Derived Peptide 31–43, but Not pα-9, Induces K562(S)-Cell Agglutination

In recent years, a growing body of evidence has highlighted the ability of some gliadin peptides, such as gliadin-derived peptide 31–43 (p31–43), to specifically elicit a mucosal innate activation in celiac duodenum as well as in intestinal epithelial cell lines (6). To assess whether p31–43 could recapitulate the surface effects of the whole gliadin digests and trigger K562(S)-cell agglutination, we incubated K562(S) cells with p31–43 or the immunodominant pα-9 gliadin peptide, ineffective in inducing an innate response (6). We demonstrated that the challenge with p31–43 induced a cellular agglutination quantitatively similar to PT gliadin digest, whereas pα-9 did not (Figure 5a,b).

As shown in Figure 6, annexin V detection by flow cytometry did not reveal apoptosis after challenge with either p31–43 or pα-9. This is in agreement with previous data that cell agglutination is a very early event, occurring within 30 min after gliadin challenge (Figure 1) in live cells (25).

P31–43 Induces Surface Events in Gliadin-Sensitive Cells

All together these findings indicate that p31–43 triggers specific mechanisms at the cell surface in K562(S) cells, thus influencing cell-to-cell interactions and cell movements. To unravel whether similar events to those described in the K562(S) model upon gliadin challenge could influence T84 collective cell migration preceding confluency, we performed two-dimensional motility experiments. In the time-lapse experiment, interactions between cells at the edges of nearby islands, such as at the extension and retraction of protrusions and the formation of apparent contacts, were observed. These interactions at the single-cell level were followed by merging of whole islands, eventually leading to cell confluency. This merging process was enhanced by the addition of p31–43, and a faster time course was observed in presence of the peptide as compared with the control (medium). In Figure 7, it can be noticed that cell islands grow faster after p31–43 addition as compared with the control T84 grown on polycarbonate filters, which form a continuous cell monolayer. The integrity of the T84 cell monolayer is a cell surface feature, regulated by some epithelial cell membrane proteins that interact with cytoskeleton (26). Gliadin peptides are known to affect the integrity of this cell monolayer, enhancing the paracellular permeability and impairing the ability to develop transepithelial resistance. So we measured the transepithelial resistance changes of the T84 monolayer after challenge with p31–43. As shown in Figure 8, the exposure of the T84 monolayer to p31–43 resulted in a significant decrease in the transepithelial resistance with respect to the cell monolayer exposed to medium alone.

DISCUSSION

Our data unravel how toxic cereals are endowed with the ability to induce a fast response in sensitive cell lines. TG2 activation is an absolute requirement to induce surface modifications and cell-to-cell interaction leading to K562(S)-cell agglutination. As TG2 enzyme activity is strictly calcium-dependent, our data also explain why the activation of such gliadin-induced cascade occurs at different times upon gluten challenge. Intracellular Ca^{2+} concentrations and TG2 protein levels are the key players of these gliadin-induced events and represent the main mechanism of the so-called nonimmune gluten toxicity. In low TG2-expressing epithelia, TG2 needs to be upregulated, whereas K562(S) cells are endowed with high protein levels and allow a prompt response to the increase in intracellular Ca^{2+} concentrations upon gliadin exposure. Our results also highlight K562(S)-cell agglutination as a new model to study the mechanisms underlying the very early events occurring at the cell surface in celiac duodenum.

These mechanisms, induced by gliadin peptides, involve the rearrangement of cytoskeleton. Changes in cytoskeleton organization upon external triggers, such as gliadin or "toxic" gliadin peptides, may activate either intracellular pathways or external signaling events responsible for cell-to-cell communication, interaction, or movements. Cell contact could in turn impact intracellular events and cell differentiation, as described in confluent intestinal epithelial cell lines (27). The confluence of cells cultured in a Petri dish may be considered the prototype of movements in a two-dimensional space. It is influenced by still undefined external stimuli as well as by cell proliferation and cytoskeleton reorganization that allow the contact and interaction between cells. In this context, K562(S) and T84 epithelial intestinal cells show a similar response upon exposure to gliadin peptides.

The relationship between gluten/gliadin and cytoskeleton has been extensively studied, as gliadin peptides induce early actin reorganization in intestinal epithelial cells (13). Gluten fractions may directly interact with actin, thus derailing actin-dependent endocytic events and altering protein and lipid composition at the brush border membrane (28,29). Our data show that the cytoskeleton reorganization induced by toxic gliadin peptides in K562(S) cells involves the Ca^{2+}-dependent activity of intracellular TG2.

It remains to be elucidated how gliadin peptides increase intracellular Ca^{2+} levels, thus triggering TG2 activation. Emerging evidences indicate that p31–43 enters intestinal epithelial cells by endocytosis, delays vesicle trafficking, and accumulates in the

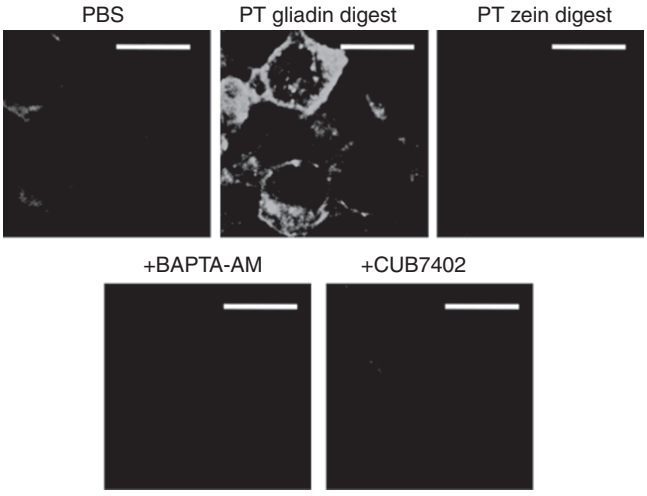

Figure 4. Actin rearrangement in K562(S) agglutinated cells. Confocal microscopy with Alexa Fluor 488 phalloidin. PT gliadin digest induces actin rearrangement in K562(S) agglutinated cells, whereas both BAPTA-AM and anti-TG2 CUB 7402 prevent the PT gliadin–induced actin rearrangement. Bars = 25 µm. BAPTA, L,2-bis(aminophenoxy)ethane-N,N,N,N′-tetraacetic acid; PBS, phosphate-buffered saline; PT, peptic tryptic; TG2, transglutaminase 2.

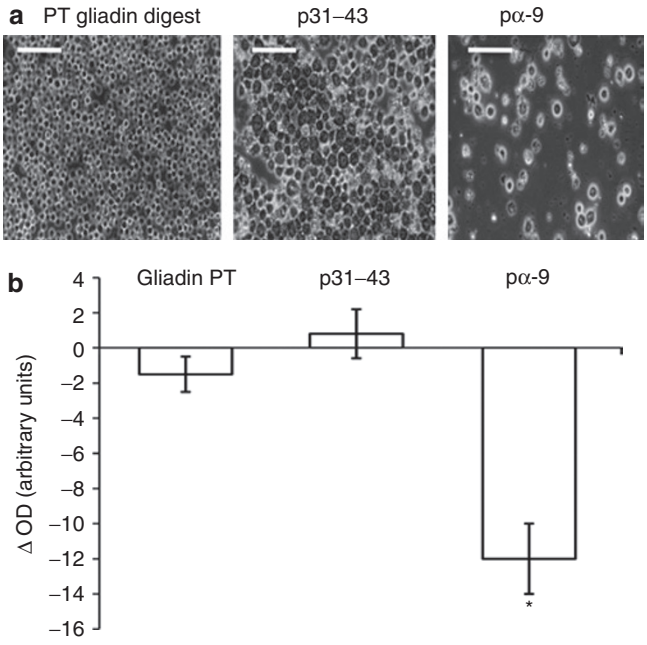

Figure 5. "Innate" gliadin peptides, not "adaptive" peptides, agglutinate K562(S) cells. (**a**) Light microscopy of K562(S) cells after 30-min incubation with PT gliadin digest, "toxic" peptide 31–43, and immunodominant pα-9 (spanning positions 57–68 of α-gliadin, pa-9). Bars = 100 µm. (**b**) Measurement of agglutination velocity. Results are expressed as mean ± SEM of three independent experiments, each performed in triplicate. Statistical significance (*$P < 0.05$) was calculated by Wilcoxon results vs. cells incubated with PT gliadin digest. OD, optical density; PT, peptic tryptic.

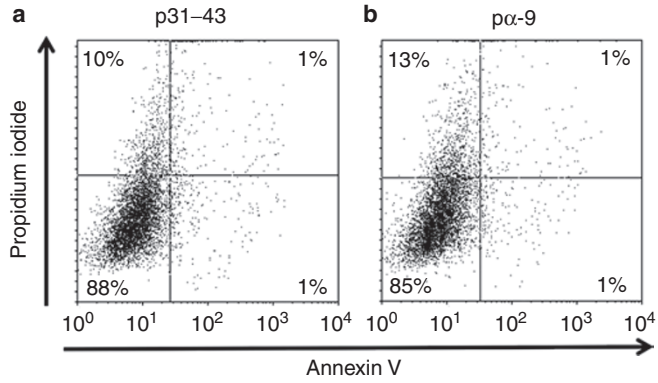

Figure 6. Gliadin peptides do not induce apoptosis in agglutinating K562(S) cells. Apoptosis of K562(S) cells was analyzed by propidium iodide and annexin V expression as described in the Methods section. (**a**) K562(S) cells cultured in the presence of gliadin-derived peptide 31–43; 1% double-positive cells and 1% single-positive cells for annexin V. (**b**) K562(S) cells challenged with pα-9; 1% cells are double positive and 1% are annexin V single positive.

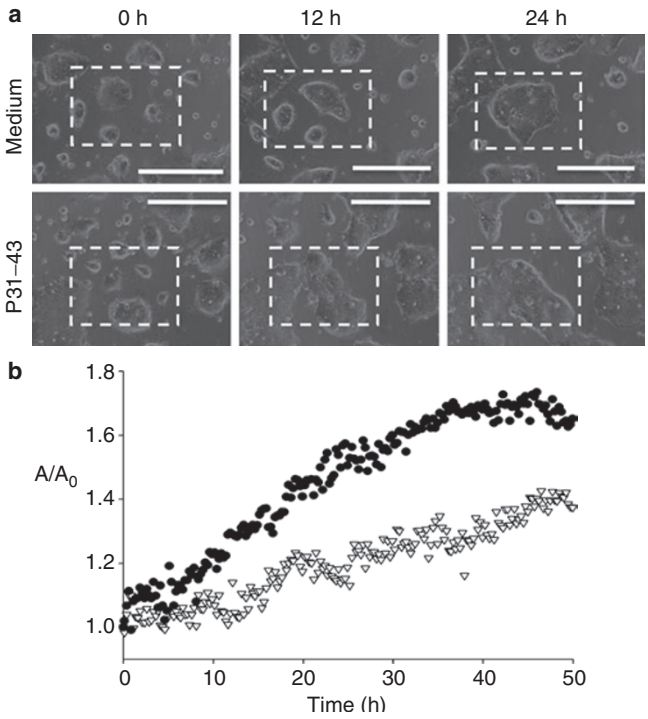

Figure 7. Cell movements of T84 cells exposed to medium or p31–43. (**a**) Two-dimensional images of T84 cells exposed to medium alone and to gliadin-derived peptide 31–43 (p31–43). Images were acquired by time-lapse video microscopy every 15 min for a total of 50 h. Bars = 300 µm. (**b**) In the plot, the area A of cell islands normalized to the initial value A_0 is shown as a function of time (inverted triangles, cells exposed to medium alone; filled circles, cells exposed to gliadin-derived peptide 31–43).

later endosomal compartments. This leads to prolonged epidermal growth factor receptor inactivation, overexpression of trans-presented interleukin (IL) 15/IL15 receptor-α complex as well as increased reactive oxygen species generation, and TG2 activation (16,30–32). Such a complex cascade of intracellular events following gliadin exposure likely derails intracellular control systems thus disrupting Ca^{2+} homeostasis by still unknown mechanisms.

Our results also validate the K562(S) agglutination test as a priceless tool for screening cereal digests and gliadin-derived peptides for toxicity in celiac patients by clarifying the mechanisms leading to agglutination. Manipulating gluten by means of chemical or enzymatic approaches, such as fungal or germinal peptidases, and searching for cereals with low toxicity (1) are emerging tools of research in CD to allow celiac patients to peacefully coexist with gluten. Therefore, the availability of a validated easy screening system of toxicity is mandatory before testing cereals with putative low toxic or detoxified gluten preparations in patients with CD.

METHODS

Materials

PT digest of bread wheat, *Triticum aestivum*, and zein of maize var. *Alijet* were obtained as previously described (8). Peptides α-9 (spanning position 57–68 of α-gliadin) and 31–43 were synthesized using fluorenylmethyloxycarbonyl (Fmoc) chemistry by Primm (Milan, Italy) (6,16). K562(S) and T84 cells were cultured as previously described (10,13).

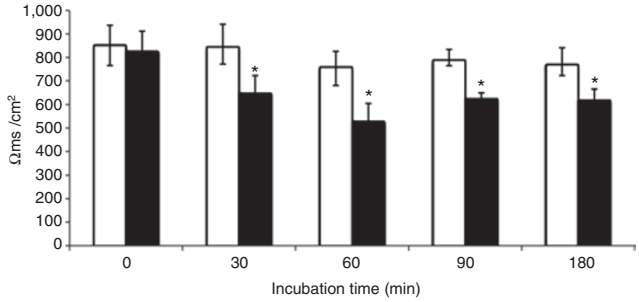

Figure 8. Measurement of TEER across the T84 monolayer exposed to medium alone (open bars) and to gliadin-derived peptide 31–43 (p31–43; black bars). Results are expressed as mean ± SEM of three independent experiments, each performed in triplicate. Statistical significance (*$P < 0.05$) was calculated by Wilcoxon results vs. cells incubated at T_0 with medium alone and p31–43. TEER, transepithelial resistance.

Agglutination Test

K562(S) cells were maintained in Roswell Park Memorial Institute medium (Gibco, Carlsbad, CA) supplemented with 10% fetal calf serum (Gibco) and subcultured every 10 d. To perform the agglutination experiments, the cells were harvested by centrifugation and washed twice with Ca^{2+} and Mg^{2+}-free PBS (Gibco). The test was performed with cells resuspended at a concentration of 10^8 cells/ml in the same PBS; 25 µl of cell suspension was added to each well of a 96-well microtiter plate containing PT gliadin or zein digest (7 mg/ml), p31–43 or pα-9 (10 µg/ml), CaCl (100 µmol/l–4 mmol/l) or ionomycin (5 mmol/l; Calbiochem, Milan, Italy). The final total volume was 100 µl. The cell suspension was incubated at room temperature for 30 min. The inhibition tests were carried out by mixing BAPTA-AM (5 mmol/l, Calbiochem) or the CUB 7402 mAb (1 mg/ml; NeoMarkers, Fremont, CA) before the addition of cells. Agglutination activity of the different peptides and molecules was measured using a 96-plate reader equipped with a stirrer (Biorad, Hercules, CA). The cell suspension turbidity was read at 600 nm (optical density 600 nm) under continuous stirring at time 0 and after 30 min. The difference of reading between T_0 and $T_{30} \times 100$ was calculated as a velocity of agglutination (33). The principle underlying this agglutination test is that turbidity associated with light scattering from suspended particles lowers upon formation of cell aggregates. Initially, sample stirring promotes cell collisions while preventing sedimentation of isolated cells. As time goes on, collision-induced cell aggregates grow in size (with a parallel decrease in turbidity) until stirring is no longer capable of keeping them in suspension. Sample agglutination takes place after sedimentation of cell aggregates at the well bottom. A typical plot of optical density as a function of time shows a lag phase followed by an exponential growth until a leveling off is reached. Both the lag phase and the final plateau time decrease with cell concentration. At 10^8 cell/ml, which is the concentration used in this work, the lag phase is negligible and steady state is reached within 30 min.

Western Blotting

K562 and T84 whole-cell extracts were prepared from cells collected and washed twice in ice-cold PBS; resuspended in 150 mmol/l NaCl, 1% Triton X-100 (Sigma, St. Louis, MO), and a mixture of protease inhibitors (1:50) (Sigma); and incubated on ice for 20 min and then centrifuged for 5 min at 4 °C. The supernatant was stored at −70 °C as whole-cell protein lysate. SDS-polyacrylamide gel electrophoresis was carried out on 4% stacking and 7.5% resolving gel (Biorad). Equal amounts of protein (50 mg) were loaded in each lane with loading buffer containing 0.1 Tris (pH 6.8), 20% glycerol, 10% mercaptoethanol, 4% SDS, and 0.2% bromophenol blue (Biorad). Samples were heated at 100 °C for 5 min before gel loading. Following electrophoresis, the proteins were transferred to a polyvinylidene fluoride membrane (Biorad). Membranes were blocked for 1 h with 5% nonfat milk in Tris-buffered saline (100 mmol/l NaCl, 5 mmol/l KCl, 100 mmol/l Tris-HCl, pH 7.4, and 0.05% Tween 20, Biorad) and incubated overnight

with TG2 antibody (mouse, clone CUB 7402; Abcam, Cambridge, MA) (1:100) and then washed three times in Tris-buffered saline, Tween, 5 min each. Secondary antibody (goat-antimouse, conjugated to horseradish peroxidase) (Biorad), was diluted 1:3,000 in the blocking solution, added to membranes for 1 h at room temperature and then washed three times in Tris-buffered saline for 5 min. Proteins on membranes were revealed by the chemiluminescence detection kit (Biorad), according to manufacturer's instructions. Intensities of protein bands on blots were evaluated using the Biorad ChemiDoc densitometer. Membranes were stripped and reprobed with β-actin antibody (Abcam) diluted 1:400 to verify equal loading of proteins.

Imaging

Intracellular calcium levels were measured in K562(S) cells using Fura-FF (Invitrogen Molecular Probes, Grand Island, NY) fluorescence ratiometric imaging. Fura FF is a low-affinity Fura that allows the measurement of levels of intracellular Ca^{2+} higher than 1 mmol/l. Briefly, the cells were loaded for 30 min at 37 °C in a hydroxyethyl-1-piperazineethanesulfonic acid (HEPES)-buffered Ringer's solution containing 4 mmol/l Fura-FF (Molecular Probes, Eugine, OR) for 40 min at room temperature. Subsequently, the cells were washed and then placed in an open-top imaging study chamber (Warner RC-10) with a bottom coverslip viewing window and the chamber attached to the microscope stage of an in Ca Imaging Workstation (Intracellular Imaging, Cincinnati, OH). Cells were imaged with a 206Nikon Super Fluor objective and regions of interest were drawn for individual cells. The Fura-FF fluorescence intensity ratio was determined by excitation at 340 nm and 380 nm and calculating the ratio of the emission intensities at 511 nm in the usual manner every 5 s. For determining the effects of gliadin and/or gliadin-derived peptides, a stable baseline for intracellular [Ca^{2+}] concentration was first obtained. Image J software (US National Institutes of Health) was used to quantify the number of cells with [Ca^{2+}] response. At least 60 cells were counted in each experiment and the values are means ± SD for five independent experiments.

TG2 activity and actin rearrangement were detected as previously described (34). Briefly, for the detection of TG2 intracellular enzymatic activity, a drop of cellular suspension of K562(S) cells treated for 30 min was put on coated slides, preincubated with TG assay buffer (965 L of 100 mmol/l Tris-HCl, pH 7.4, 25 ml of 200 mmol/l $CaCl_2$, both from Sigma) for 15 min, and then preincubated with the same triglyceride assay buffer added with 10 µl of 10 mmol/l biotinylated monodansylcadaverine (Molecular Probes, Leiden, The Netherlands) for 1 h at room temperature. The reaction was stopped with 25 mmol/l EDTA for 5 min; the slides were then fixed in 4% paraformaldehyde for 10 min. The incorporation of labeled substrate was visualized by incubation with R-phycoerythrin-conjugated streptavidin (1:50; Dako, Glostrup, Denmark) for 30 min. Control experiments included the omission of biotinylated monodansylcadaverine and replacement of 200 mmol/l $CaCl_2$ with 200 mmol/l EDTA (Sigma).

Detection of T84 Collective Migration

T84 cells were plated on multiwell culture dishes with glass bottom (Ibidi, Martinsried, Germany). After 48 h, cells were incubated with 40 µg/ml of p31–43, and the dish was placed in a time-lapse video microscopy workstation (35). The system was equipped with an inverted optical microscope (Zeiss, Obercoken, Germany) enclosed in a plexiglass cage where a prewarmed air stream at 37 °C mixed with CO_2 was circulated to mimic the conditions of a bench incubator for cell cultures. The microscope was connected to a high-resolution video camera. To follow T84 collective migration, images were iteratively acquired at several locations within the sample by using a motorized x–y stage and focus control. The time delay between the acquisition of consecutive images was 15 min, for a total of 50 h.

Flow Cytometry

K562(S) cells were incubated with fluorescein isothiocyanate–conjugated annexin V (BD Pharmigen, San Jose, CA). Labeling procedures were performed according to the manufacturer's instructions. Briefly, cells were resuspended in annexin labeling solution containing 10 mmol/l HEPES (pH 7.4), 140 mmol/l NaCl, 5 mmol/l $CaCl_2$, and fluorescein-conjugated annexin V for 15 min. After being washed twice with PBS, cell pellets were resuspended in a solution of PBS with propidium iodide (2 mg/ml) and analyzed by flow cytometry (Partec, Munich, Germany). Data were analyzed with WinDMI software, Topsham, ME.

Measurement of Transepithelial Electric Resistance in T84 Monolayer

Transepithelial electrical resistance of T84 cell monolayers was measured using a Millicell ERS device (Millipore, Bedford, MA). Cells were seeded on polycarbonate inserts (0.45 mm pore diameter, 0.9 cm^2 area) (BD Falcon, Franklin Lakes, NJ) and left to differentiate for 19 d. The cells were treated with p31–43 (40 µg/ml) up to 3 h.

Statistical Analysis

Treated cells were compared with those cultured in medium alone. All experiments were performed at least in triplicate. Data distribution was analyzed, and statistical differences were evaluated using the Wilcoxon test and SPSS 12 software, Armonk, NY. A P value of <0.05 was consid-ered significant.

REFERENCES

1. Schuppan D, Junker Y, Barisani D. Celiac disease: from pathogenesis to novel therapies. Gastroenterology 2009;137:1912–33.
2. Kagnoff MF. Celiac disease: pathogenesis of a model immunogenetic disease. J Clin Invest 2007;117:41–9.
3. Green PH, Cellier C. Celiac disease. N Engl J Med 2007;357:1731–43.
4. Londei M, Ciacci C, Ricciardelli I, Vacca L, Quaratino S, Maiuri L. Gliadin as a stimulator of innate responses in celiac disease. Mol Immunol 2005;42:913–8.
5. Meresse B, Ripoche J, Heyman M, Cerf-Bensussan N. Celiac disease: from oral tolerance to intestinal inflammation, autoimmunity and lymphomagenesis. Mucosal Immunol 2009;2:8–23.
6. Maiuri L, Ciacci C, Ricciardelli I, et al. Association between innate response to gliadin and activation of pathogenic T cells in coeliac disease. Lancet 2003;362:30–7.
7. Giovannini C, Sanchez M, Straface E, Scazzocchio B, Silano M, De Vincenzi M. Induction of apoptosis in caco-2 cells by wheat gliadin peptides. Toxicology 2000;145:63–71.
8. De Ritis G, Occorsio P, Auricchio S, Gramenzi F, Morisi G, Silano V. Toxicity of wheat flour proteins and protein-derived peptides for *in vitro* developing intestine from rat fetus. Pediatr Res 1979;13:1255–61.
9. Silano M, De Vincenzi M. *In vitro* screening of food peptides toxic for coeliac and other gluten-sensitive patients: a review. Toxicology 1999;132:99–110.
10. De Vincenzi M, Stammati A, Luchetti R, Silano M, Gasbarrini G, Silano V. Structural specificities and significance for coeliac disease of wheat gliadin peptides able to agglutinate or to prevent agglutination of K562(S) cells. Toxicology 1998;127:97–106.
11. Silano M, Dessì M, De Vincenzi M, Cornell H. *In vitro* tests indicate that certain varieties of oats may be harmful to patients with coeliac disease. J Gastroenterol Hepatol 2007;22:528–31.
12. Clemente MG, De Virgiliis S, Kang JS, et al. Early effects of gliadin on enterocyte intracellular signalling involved in intestinal barrier function. Gut 2003;52:218–23.
13. Maiuri L, Ciacci C, Ricciardelli I, et al. Unexpected role of surface transglutaminase type II in celiac disease. Gastroenterology 2005;129:1400–13.
14. Fesus L, Piacentini M. Transglutaminase 2: an enigmatic enzyme with diverse functions. Trends Biochem Sci 2002;27:534–9.
15. Collighan RJ, Griffin M. Transglutaminase 2 cross-linking of matrix proteins: biological significance and medical applications. Amino Acids 2009;36:659–70.
16. Luciani A, Villella VR, Vasaturo A, et al. Lysosomal accumulation of gliadin p31-43 peptide induces oxidative stress and tissue transglutaminase-mediated PPARgamma downregulation in intestinal epithelial cells and coeliac mucosa. Gut 2010;59:311–9.
17. Villanacci V, Not T, Sblattero D, et al. Mucosal tissue transglutaminase expression in celiac disease. J Cell Mol Med 2009;13:334–40.

18. Silano M, De Vincenzi M. Bioactive antinutritional peptides derived from cereal prolamins: a review. Nahrung 1999;43:175–84.
19. Dieterich W, Trapp D, Esslinger B, et al. Autoantibodies of patients with coeliac disease are insufficient to block tissue transglutaminase activity. Gut 2003;52:1562–6.
20. Gawaz M, Ott I, Reininger AJ, Heinzmann U, Neumann FJ. Agglutination of isolated platelet membranes. Arterioscler Thromb Vasc Biol 1996;16:621–7.
21. Király R, Csosz E, Kurtán T, et al. Functional significance of five noncanonical Ca2+-binding sites of human transglutaminase 2 characterized by site-directed mutagenesis. FEBS J 2009;276:7083–96.
22. O'Neill GM, Prasanna Murthy SN, Lorand L, et al. Activation of transglutaminase in mu-calpain null erythrocytes. Biochem Biophys Res Commun 2003;307:327–31.
23. Painter RG, Ginsberg M. Concanavalin A induces interactions between surface glycoproteins and the platelet cytoskeleton. J Cell Biol 1982;92:565–73.
24. Vlodavsky I, Sachs L. Difference in the calcium regulation of concanavalin A agglutinability and surface microvilli in normal and transformed cells. Relationship to membrane–cytoskeleton interaction. Exp Cell Res 1977;105:179–89.
25. Yagi M, Campos-Neto A, Gollahon K. Morphological and biochemical changes in a hematopoietic cell line induced by jacalin, a lectin derived from *Artocarpus integrifolia*. Biochem Biophys Res Commun 1995;209:263–70.
26. Quaroni A, Beaulieu JF. Cell dynamics and differentiation of conditionally immortalized human intestinal epithelial cells. Gastroenterology 1997;113:1198–213.
27. Drago S, El Asmar R, Di Pierro M, et al. Gliadin, zonulin and gut permeability: Effects on celiac and non-celiac intestinal mucosa and intestinal cell lines. Scand J Gastroenterol 2006;41:408–19.
28. Reinke Y, Behrendt M, Schmidt S, Zimmer KP, Naim HY. Impairment of protein trafficking by direct interaction of gliadin peptides with actin. Exp Cell Res 2011;317:2124–35.
29. Reinke Y, Zimmer KP, Naim HY. Toxic peptides in Frazer's fraction interact with the actin cytoskeleton and affect the targeting and function of intestinal proteins. Exp Cell Res 2009;315:3442–52.
30. Barone MV, Zanzi D, Maglio M, et al. Gliadin-mediated proliferation and innate immune activation in celiac disease are due to alterations in vesicular trafficking. PLoS ONE 2011;6:e17039.
31. Barone MV, Nanayakkara M, Paolella G, et al. Gliadin peptide P31-43 localises to endocytic vesicles and interferes with their maturation. PLoS ONE 2010;5:e12246.
32. Barone MV, Gimigliano A, Castoria G, et al. Growth factor-like activity of gliadin, an alimentary protein: implications for coeliac disease. Gut 2007;56:480–8.
33. Ohba H, Toyokawa T, Yasuda S, Hoshino T, Itoh K, Yamasaki N. Spectroscopic analysis of the cytoagglutinating activity of abrin-b isolated from *Abrus precatorius* seeds against leukemic cells. Biosci Biotechnol Biochem 1997;61:737–9.
34. Luciani A, Villella VR, Vasaturo A, et al. SUMOylation of tissue transglutaminase as link between oxidative stress and inflammation. J Immunol 2009;183:2775–84.
35. Fico A, Manganelli G, Simeone M, Guido S, Minchiotti G, Filosa S. High-throughput screening-compatible single-step protocol to differentiate embryonic stem cells in neurons. Stem Cells Dev 2008;17:573–84.